N72-24812

NASA TECHNICAL MEMORANDUM

NASA TM X- 68026

NASA TM X- 68026

EXHAUST FLOW AND PROPULSION CHARACTERISTICS OF A PULSED MPD ARC THRUSTER

by Charles J. Michels
Lewis Research Center
Cleveland, Ohio

and

Thomas M. York
Pennsylvania State University
University Park, Pennsylvania

TECHNICAL PAPER proposed for presentation at
Ninth Electric Propulsion Conference sponsored by
the American Institute of Aeronautics and Astronautics
Washington, D. C., April 17-19, 1972

EXHAUST FLOW AND PROPULSION CHARACTERISTICS OF A PULSED MPD ARC THRUSTER

Charles J. Michels
Lewis Research Center
Cleveland, Ohio

and

Thomas M. York
Pennsylvania State University
University Park, Pennsylvania

Abstract

Experimental investigation of the near-field, megawatt, single-shot exhaust is presented for the self-field and auxiliary field cases (0-2 T). Plasma impact pressure and number density are correlated to provide velocity profiles ($3x10^4$ to $7x10^4$ m/sec), thrust (10 to 120 N), impulse (3 to 16 N-sec) and mass accounting. The data agree with Hügel's self-field theory for the case where thrust is produced entirely by electromagnetic force. The data show that the thrust monatonically increases with auxiliary field.

E-6832

Introduction

A better understanding of acceleration mechanisms and propulsion characteristics of MPD-Arc thrusters operating from subkilowatt to megawatt power levels is needed to evaluate their usefulness for propulsion. This paper presents the results of an experimental investigation of the near-field megawatt MPD-Arc exhaust flow.

Measurement of exhaust impact pressure was undertaken to more directly determine thruster-related performance. The earliest impact pressure measurements were described in reference 1. This work identified the starting transients that dominated the pulsed discharge event for at least 100 microseconds prior to any quasi-steady plasma flow in the exhaust. These measurements showed a large amplitude initial pressure pulse followed by lower order pressure signals that were not well understood. The present effort was directly primarily toward diagnosis of the pressure in the "after" time period, i.e., after the initial pulse has passed the probing station. The initial pulse has been associated with relatively cold and weakly-ionized flow, while the "after" region of flow is now established[2] as more fully ionized plasma. A NASA supported effort[3] resulted in the development of a tailored pressure probing unit for use in the rarefied plasma exhaust flow of the "after" time period. Early measurements with this probe on centerline in the exhaust duct, 30 cm downstream from the anode face probe unit are described in reference 4.

The new impact pressure data obtained with this probe are combined with earlier reported experimental electron density and temperature data[2,5] to provide calculated values of the exhaust velocity. Integrating the new pressure data over the exhaust area yields a calculated instantaneous thrust and impulse bit. The impact pressure and density data are further analyzed to determine the instantaneous mass flow rate in the plasma exhaust. An accounting is given of mass apportioned to the initial cold gas flow, the starting transient flow, and the plasma flow portions of the exhaust. The role of propulsion parameters and comparison with theories[6,7] for the self-field and auxiliary magnetic field[8] modes of operation of the thruster are discussed.

Apparatus

Capacitor Bank and Switch System

The arc was energized by a 10 kilojoule capacitor bank, described in detail in reference 5. The discharge was initiated after the bank switch was closed and arc current was allowed to develop to its peak value. Then (21 μsec after bank firing time) a crowbar switch was closed, forcing current to decay monatonically with time. The L/R decay time ranged from 250 to 350 microseconds depending on arc resistance. This circuitry allowed an almost linear decay of arc current for 500 microseconds after crowbarring time. It is during this time period that the data was gathered. Typical voltage and current waveshapes for the two peak current cases investigated (11.2 and 20.0 kA) are shown in figure 1. Distinctly different waveshapes are evident for each of the three values of auxiliary magnetic field (0, 1, and 2 T) applied in the magnetic nozzle configuration.

Arc Chamber System

A cross-sectional view of the arc chamber is shown in figure 2. A superconducting magnet is used to supply an auxiliary magnetic field at the arc chamber which can be varied from 0 to 2.0 T. An iron filings map of the magnetic field is also shown. The cathode is a tungsten ribbon measuring 1 cm wide, 2 cm long, and 1 mm thick. The anode is a 4.2 cm inside diameter copper ring.

Nitrogen gas was introduced into the arc chamber by a high speed gas valve that was operated by an electromagnetic actuator. All tests were run with the same puff mass at a peak nitrogen cold flow rate of 3 g/sec. The transient cold flow gas pressure in the arc chamber was measured by a commercially available piezoelectric pressure transducer in a previous experiment. That pressure and the orifice equations for steady flow were used to calculate the mass flow rate for all the tests of this report. From the transient pressure records it was found that stable flow occurred after 650 microseconds. The arc was started at that time.

Thereafter, the transient plasma flows for a few hundred microseconds into the evacuated glassware section.

A sequence controller actuates gas puff injection, delay for gas distribution, bank switch closure, crowbar switch closure, and then data gathering "start" times. The system can be recycled every 4 minutes.

Piezoelectric Pressure Probe

Basic considerations relating to the measurement of pressure in a flowing plasma have been previously reported.[1,9] A new probing unit was specifically developed[3] for the present exhaust conditions. The geometry of piezoelectric sensing element, related support structure, and electrical circuitry were designed for the magnitude and duration of the pressure signals anticipated and a matched sensing unit was utilized as a built-in simultaneous accelerometer. Two probing units with 0.75 and 1.25 cm diameter sensing surfaces and 2.0, 2.5 cm o.d. housing respectively, were constructed. Calibration was carried out with a simple shock tube. In both cases, with 1.8 m of coaxial cable, an output of 4 volts per atmosphere was achieved; with a matched amplifier (x10), an output of 40 volts per atm resulted. In order to more precisely define trends in the pressure data, an electronic low-pass filter (Spectrum Analog Electronic Filter Type H-18) was used at times for the 0.7 cm probing unit as it demonstrated an active, well-defined higher frequency stress oscillation after impact of the pressure front. Corrections were made for the slight delay of the filter (~10 μsec).

A rigid mounting of the probe support fitting and subsequent comparison of simultaneous records from the pressure sensing and built-in accelerometer units revealed pressure signals an order of magnitude higher than those due to undesirable probe accelerations. However, extraneous signals due to thermal effects and probe heating proved to be substantial. Experimental evaluation indicated that radiant energy flux from both the source and local plasma radiation produced insignificant effects. However, thermal conduction to the probe from the plasma proved to be dominant. A single layer of vinyl electrical insulating tape (Scotch Brand No. 22, 3M Mfg. Co.) covering the sides and sensing surface of the probe eliminated the thermal drift without degrading pressure sensitivity or linearity of response.

Results and Discussions

Cold Flow Total Pressure

The piezo-pressure probe was used to measure "cold" gas flow in the duct. The propellant was injected without starting the arc. At the data gathering times and station used in this report, the cold gas propellant stagnation pressure is an order of magnitude less (about 6 N/m^2 maximum) than the measured pressures for the powered case. Supplementary measurements indicate static pressures are approximately one-tenth of this stagnation pressure.

Exhaust Pressure Profiles

As outlined in reference 1, the sequence of events at a given station in the exhaust for a single shot megawatt-level arc source is:

(a) Exhaust light arrival (about 70 μsec after arc initiation at 30 cm).

(b) A few microseconds later, a narrow (20 to 70 μsec) total pressure pulse of neutral gas passes, most probably blast wave related.

(c) Arc current exhaust (plume) arrives tens of microseconds later, at the approximate time that plasma is first detected.

(d) A flowing plasma is noted.

This sequence can be correlated with time variations of the exhaust impact pressure shown in figure 3 for a station 30 cm downstream from the anode. The pressure was measured with the 0.75 cm diameter piezo probe for the case where the peak current is 11.2 kA and for various auxiliary magnetic fields, 0, 1.0 and 2.0 tesla. The figure shows the time-varying impact pressure at three different radii (0, 2, and 4 cm).

Each trace shown is the mean value of two superimposed traces and has been smoothed so that the internal stress oscillations of the piezo probe are not shown. Some shot to shot variation in data records exists as was shown in the raw data (two-shot overlays) of reference 4.

The data presented in figure 3 show one common feature, the total pressure appears as an initial large amplitude pulse (8-10,000 N/m^2, 20 to 70 μsec wide) with lower and varying pressure (1-2000 N/m^2) thereafter for 200 microseconds. The initial pulse, as in earlier work[1] describing this phenomenon, is most probably attributable to a blast wave generating weakly ionized gas. The exact nature of the blast wave-like period remains to be determined. A similar effect has been noted[10] in a pinch experiment. The present report is concerned primarily with the period of time after the initial pulse; that is, the plasma flow period.

All the data of figure 3, after the initial pressure front show a drop and subsequent recovery to another maximum impact pressure. The recovery time, T_1, is defined as the time to reach 63 percent (e - folding time) of the peak plasma flow impact pressure. It is the time to establish a period of quasi-steady plasma exhaust flow. Table I lists values of the recovery time.

Table I - Recovery Times

T_1(μsec)	B(T)	I_{max}(kA)
250	0	11.2
210	1	11.2
200	2	11.2
225	0	20.0
200	1	20.0
175	2	20.0

Radial Profiles

11.2 kA Case - The radial variation of the peak value of the initial pulse (blast wave part) as shown in figure 3 is much the same as in reference 1 (fig. 13). The dependence of peak value on auxiliary magnetic field is also much the same. The new information concerns the radial pressure variation vs time for the plasma flow portion of the exhaust flow. For the B = 0 case (fig. 3(a)), the plasma flow pressure profile decays with radius, the maximum pressure being on centerline. By contrast, for the B = 1.0 T case (fig. 3(b)), the plasma flow pressure increases with radius. At B = 2.0 T, the plasma flow pressure profile is also seen to increase with radius, but with generally less pronounced amplitude change than for B = 1.0 T. Increasing the auxiliary magnetic field to 2.0 T has generally reduced the amplitude of the plasma pressure profiles. For both magnetic nozzle cases, the pressure on centerline is less than for the self-field case. The "hole" (or reduced density) in the exhaust on centerline was first described in terms of number density in reference 5 (through a Thomson scattering measurement). It is now manifest as a reduction in pressure on centerline. The peak value of plasma flow pressure is generally less than half the peak value of the blast wave pressure pulse. After the peak value of plasma flow pressure, the pressure decays with time as does the arc current. Although not presented, the static pressure profiles are at least an order of magnitude smaller than the corresponding impact pressure.

20 kA Case - Figure 4 shows the temporal variation of the exhaust impact pressure at Z = 30 cm for the 20 kA peak current case. Data are shown for the same auxiliary magnetic fields and radial positions as in figure 3. The general characteristics described for figure 3 are also evident at this higher peak current. The primary differences are in the fact that the pressures are approximately twice as large for the 20 kA case and the recovery time, T_1, is less.

Exhaust Velocity Calculations

The velocity of the blast wave portion of the exhaust was calculated and described in reference 1. This velocity was determined by the time of flight of the pulse past two measuring stations in the duct. At Z = 30 cm, the velocities were about 2×10^4 m/sec for the 11.2 kA, B = 0 case. With applied magnetic field the radial profiles of the velocity became inverted. The reader is referred to reference 1 for more details.

The pressure data of the present report can be combined with the number density data of reference 2 to provide a calculated velocity at each instant of time for the plasma flow portion of the exhaust. The calculation assumes complete ionization and that $P = \rho V^2$, where P is the impact pressure, ρ is the density, and V is the velocity. An exact analysis of the pressure-velocity relationship in the flowing exhaust plasma must include detailed plasma sheath and gasdynamic effects. Meaningful evaluation of such higher order interactions would require more instrument precision and experiment repeatability than is presently available. Corrections to the pressure data because of flow angularity, velocity gradients, etc., are estimated to be negligible within the accuracy of the experiment. The velocities calculated prior to 150 microseconds are not considered to be a part of the true "blowing" plasma flow phase of the exhaust since the partially ionized blast wave-like decay pressure may overlap the plasma flow pressure at times earlier than 150 microseconds. This makes the calculation of velocity difficult to interpret.

Velocity Profiles for the Self-Field Case - The results of the velocity calculation for the two different current cases, 11.2 kA and 20.0 kA, are presented in figure 5. In figure 5(a), calculations are shown only for two radii (r = 0, and r = 2 cm) because number density data at r = 4 cm was below the instrument detectability limit ($<10^{13}$ cm^{-3}). The velocity in the plasma flow portion of the exhaust at about 250 microseconds is 3.5×10^4 m/sec. This is an order of magnitude larger than the blast wave velocity (see ref. 1). A steady flow at this velocity would correspond to a specific impulse of about 3500 seconds.

For the 20.0 kA case shown in figure 5(b), pressure and number density data were available for three radial locations (r = 0, 2, and 4 cm). In general, the velocities are larger in magnitude and the exhaust duration is longer (450 μsec). The velocity is lower toward the duct edge and decreases faster. Generally, the velocities agree with theoretical calculations described by Hügel (ref. 7, fig. 3).

Further analysis of the temporal variations in the sustained plasma flow is not considered warranted at present because the 15 cm duct may not be adequate to avoid wall interactions. The thruster is scheduled to operate in a much larger free exhaust facility in the near future.

Velocity Profiles for the Auxiliary Field Case - The influence of the auxiliary magnetic field on the plasma flow velocity is shown in figure 6. The data are presented for one radius (r = 4 cm) because even though the pressure data are available for other radii, the number density was below the detectable limit (1×10^{13} particles/cm^3). In figure 6(a) (11.2 kA peak current), the velocity for the B = 2.0 T field case is less than the velocity for the B = 1.0 T field case. It should be noted that even though the arc power is greater for the 2.0 T case, the arc current probably is not sufficient to provide an optimum condition for this mass input. This condition is more dramatically noted when thrust is analyzed in later sections of this report.

For the 20 kA peak current case (fig. 6(b)), the velocity increases with auxiliary magnetic field, that is with arc power. At recovery time, T_1, the equivalent steady-flow specific impulse for the data of figure 6(b) are on the order of 2700 seconds for the B = 0 case, 5300 seconds for the B = 1.0 T case, and 6500 seconds for the B = 2.0 T case.

Thrust and Impulse Bit

The benefits of pressure probing in the plasma

flow portion of the exhaust become most evident when the impact pressure measurements versus radius and time are integrated over the exhaust area to provide a critical propulsion parameter, namely thrust. The excellent high frequency response of the probe allow instantaneous thrust determinations, a difficult feat for most reaction thrust measuring systems.

The thrust varies with time during a typical single-shot event. The initial thrust (a few newtons) is caused by cold gas propellant flow out the exhaust nozzle prior to arc start-up. Then there is a time-varying but larger thrust as the arc is ignited. This is associated with the blast wave-like transient in the flow. Both the cold gas thrust and the blast wave-like thrust can be considered starting transients. In reference 1 it was pointed out that if the arc powering time is short, the impulse provided by the starting transient thrust will dominate over the impulse due to the later plasma flow portion of the thrust cycle. Attempting to apply steady state plasma accelerator theory to that short pulse case obviously would result in errors. Following the starting transient thrust there is a time varying thrust caused by the plasma flow portion of the exhaust. This portion of the thrusting time can be related more closely to steady thruster performance.

Instantaneous thrust versus time for the case of a peak current of 11.2 kA is shown in figure 7. The peak thrust values vary from 25 to 40 newtons, depending on auxiliary field case. Although input power levels increase with increasing magnetic field, thrust does not increase monatonically with auxiliary magnetic field. The time integral of the thrust for the plasma flow portion of the exhaust is shown to yield impulses of 3.4 to 6.1 mN-sec. In sharp contrast to the 11.2 kA case, the instantaneous thrust vs time data for 20 kA peak current is monatonically increasing with the value of the auxiliary magnet field. As the peak arc power increases from 3.0 to 7.2 megawatts, the peak thrust increases from 73 to 120 newtons. Impulse bit also increases with magnetic field from 8 to 16 mN-sec.

Mass Accounting

The cold flow of gas for a single shot has been analyzed by measuring the pressure in the arc chamber and the mass flow has been calculated from the sonic flow equations for mass flow through the 4.12 cm diameter anode. The transient arc chamber pressure is noted to reach a peak value of 0.15 psia at about 600 μsec after the 70 μsec puff of N_2 has been introduced into the evacuated arc chamber. This value indicates a flow rate of 3.0 gms/sec when the arc is initiated. The measured arc chamber pressure for the cold flow case after peak pressure is simply an exponential decay of pressure with time. In figure 9, mass flow rate versus time is shown for three cases. The upper curve is the indicated cold flow rate, determined by the above procedure, shown decaying with time. At 200 μsec after the discharge is initiated (850 μsec after the initial puff of gas was introduced into the chamber) the flow rate is seen to be about 2.0 gs/sec. By the time the exhaust flow event would normally be over (400 μsec of arc initiation) the mass flow rate is down to 1.5 gs/sec.

The remaining two curves in figure 9 represent measured ion mass flow rates during the active thrusting plasma flow period. These instantaneous flow rates were determined from temporal variations in ion number density obtained from an earlier Thomson scattering experimental measurement[2] and the velocities calculated from pressure data in the present paper. The flow rates were calculated for the B = 0 auxiliary field case, for 11.2 kA peak current and 20 kA peak current cases. For the more optimum case, 20 kA peak current, the mass flow rates for 150 to 225 μsec period are in good agreement with cold mass flow rate, indicating fair mass utilization. For the 11.2 kA peak current case there is a large difference between cold flow mass flow rate and that calculated to be occurring in the plasma flow portion of the exhaust. This indicates poor mass utilization and is another indication of the off-optimum operation for this low-current case. The total mass per shot is obtained by measuring the increase in static pressure when the cold flow of gas is allowed to fill the arc chamber and 90 liter glassware exhaust duct system that has been closed off from the vacuum pump. This mass per shot is measured to be 3000 micrograms.

Using the above data, Table II represents the mass accounting for various time increments for a typical shot.

Table II - Mass Accounting

(B = 0, 20 kA)

Event	% of Total Mass Involved	Mass in Micrograms
Cold gas flow before arc is "on" (measured)	33	1000
"Blast wave" flow (measured)	3	100
Plasma flow portion of exhaust (measured)	8	250
Unaccounted for flow	15	450
"Bleedout" of mass after powering cycle	41	1200
Total mass measured	100%	3000

The mass accounting shows that 33% of the mass per shot is expended in developing the proper mass flow rate (3 g/sec) before the arc is ignited. The "bleedout" of mass after the powering cycle is 41% of the mass per shot. During the powering cycle, 3% of the mass is measured in the "blastwave" part and 8% is measured in the plasma flow portion of the exhaust. This leaves 15% of the total mass unaccounted. The unaccounted mass is the measured difference of the integrated cold flow mass and the

integrated plasma flow mass in figure 9. It is not resolved whether this is due to uncertainty in the measurements or due to mass not properly utilized in the thruster.

Propulsion Parameters - Experiment and Theory

In order to clarify the basic regimes of thruster operation, the instantaneous thrust data (fig. 8) were correlated with the instantaneous discharge current of figure 1. The results are presented in figure 10 for the 20.0 kA peak current case; the variation of instantaneous thrust with arc current is shown, with auxiliary magnetic field as an additional parameter. Time during the discharge event is noted to progress downward in figure 10 for each case, and accordingly, the mass flow rate is maximum at the peak thrust values and decreases with time (fig. 9). Data error bars are not presented, but could be 20 percent of the indicated values. Also presented for reference in figure 10 is the variation of self-field electromagnetic thrust versus current, calculated using the standard analytic formulation.[7,12] The cathode spot size used in the calculation was estimated from erosion patterns and assumed constant. However, the curves shown are clearly not straight lines (exponential relationship of thrust to current) over the range of experimental current conditions. The period of higher current flow with B = 0 is seen to agree reasonably well with that analytical formulation. Periods of apparently quasi-steady plasma flow are identified by the solid curves. The data shown clearly emphasizes the role that an auxiliary magnetic field can play in increasing thrust for a given value of discharge current. Specifically, taking a value of discharge current of 7 kA, the variation of thrust derived from the integrated exhaust measurements versus the magnitude of the applied magnetic field is presented in figure 11. Thrust is noted to monatonically increase with auxiliary magnetic field. However, the increasing value of applied magnetic field can be shown (fig. 1) to increase the power level of the arc thruster discharge; the variation of discharge power with magnetic field is presented as a second curve in figure 11. The ratio of thrust to power is increasing with magnetic field. Hence, the efficiency is also increasing with applied field. The efficiency is not calculated because of uncertainties in the mass flow rate discussed earlier.

The condition of criticality for current and mass flow rate described in reference 13 is

$$\left(\frac{I^2}{\dot{m}}\right)_{crit.} \approx \frac{2\ eV_i}{bm}$$

where e is the electronic charge, V_i is the ionization potential, m is the mass of the particles and b is a constant of the thruster. The value of $I^2/\dot{m}$ for the 20 kA self-field case varies from 25 to 200. In reference 13 the critical value of this parameter was given as between 60 and 150 for somewhat similar propellants and geometry. The value depends on whether instantaneous cold flow rate or instantaneous plasma flow rate is used and on the range of uncertainty of the measured mass flow rate.

Conclusions

The results of an experimental investigation of the near-field megawatt MPD-Arc exhaust flow are presented. The thruster was operated single-shot and results were obtained with and without auxiliary magnetic field. The data consists of measurements of impact pressure with a newly designed piezo pressure probe system and of plasma density determined in earlier work. The data were analyzed to determine propulsion characteristics such as thrust, impulse bit, velocity, and mass accounting. Conclusions for this study are as follows:

1. New impact pressure data reconfirm the initial starting transient pressure pulse and add new radial and temporal profile data for the later occurring plasma flow part of the exhaust. These impact pressures varied from 1×10^3 to 4×10^3 N/m^2 for the few hundred microseconds duration of the plasma flow portion for the self-field and for B = 1.0 T and B = 2.0 T auxiliary field cases.

2. Calculated exhaust velocity during the plasma flow period varied from 2×10^4 to 7×10^4 m/sec and were functions of radial position, as well as auxiliary magnetic field. For the self-field case, the experimentally determined velocities agree with Hügel's theory for the case where acceleration is produced entirely by electromagnetic force.

3. For the self-field case, although the thrust varies with time under the influence of decaying current and mass flow rate, there is a region which approaches the steady-flow thrust (proportional to current squared).

4. Thrust is found to increase monatonically with auxiliary magnetic field. Impulse bit was found to range from 3 to 16 N sec, dependent on magnetic field strength.

References

1. Michels, C. J. and York, T. M., "Pressure Measurements in the Exhaust of a Pulsed Megawatt MPD ARC Thruster," Paper 71-196, Jan. 1971, AIAA, New York, N.Y.

2. Michels, C. J., Rose, J. R., and Sigman, D. R., "Temporal Survey of Electron Number Density and Electron Temperature in the Exhaust of a Megawatt MPD-Arc Thruster," Paper 72-209, Jan. 1972, AIAA, New York, N.Y.

3. York, T M., "Dynamic Pressure Transducer System for Pulsed Plasma Flow Diagnosis," AERSP 71-3, June 1971, Pennsylvania State Univ., University Park, Pa.

4. Michels, C. J. and York, T. M., "Flow Characteristics in the Exhaust of a Pulsed Megawatt Gas Fed Arc," TM X-67931, 1971, NASA, Cleveland, Ohio.

5. Michels, C. J. and Sigman, D. R., "Exhaust Characteristics of a Megawatt Nitrogen MPD-ARC Thruster," AIAA Journal, Vol. 9, No. 6, June 1971, p. 1144-1147

6. Jahn, R. G., Clark, K. E., Oberth, R. C., and Turchi, P. J., "Acceleration Patterns in Quasi-Steady MPD Arcs, AIAA Journal, Vol. 9, No. 1, Jan. 1971, pp. 167-172.

7. Hügel, H., Kruelle, G., and Peters, T., "Investigations on Plasma Thrusters with Thermal and Self-Magnetic Acceleration," AIAA Journal, Vol. 5, No. 3, Mar. 1967, pp. 551-558.

8. John, R. R., Bennett, S., and Connors, J. F., "Experimental Performance of a High Specific Impulse Arc Jet Engine," Astronautica Acta, Vol. 11, Mar.-Apr. 1966, pp. 97-103.

9. York, T. M., "Stress Dynamics in High Speed Piezoelectric Pressure Probes," Review of Scientific Instruments, Vol. 41, No. 4, Apr. 1970, pp. 519-521.

10. York, T. M. and Stover, E. K., "Transient Flow and Heating Characteristics in a Pinched Plasma Column," Paper 72-208, Jan. 1972, AIAA, New York, N.Y.

11. Michels, C. J., "Dynamic Voltage-Current Characteristics of a Megawatt MPD-ARC Thruster," AIAA Journal, Vol. 9, No. 1, Jan. 1971, pp. 173-176.

12. Hügel, H., "Self-Magnetic Effect in Arcjet Engines" AIAA Journal, Vol. 6, No. 8, Aug. 1968, pp. 1573-1575.

13. Malliaris, A. C., John, R. R., Garrison, R. L., and Libby, D. R., "Performance of Quasi-Steady MPD Thrusters at High Powers," AIAA Journal, Vol. 10, No. 2, Feb. 1972, pp. 121-122.

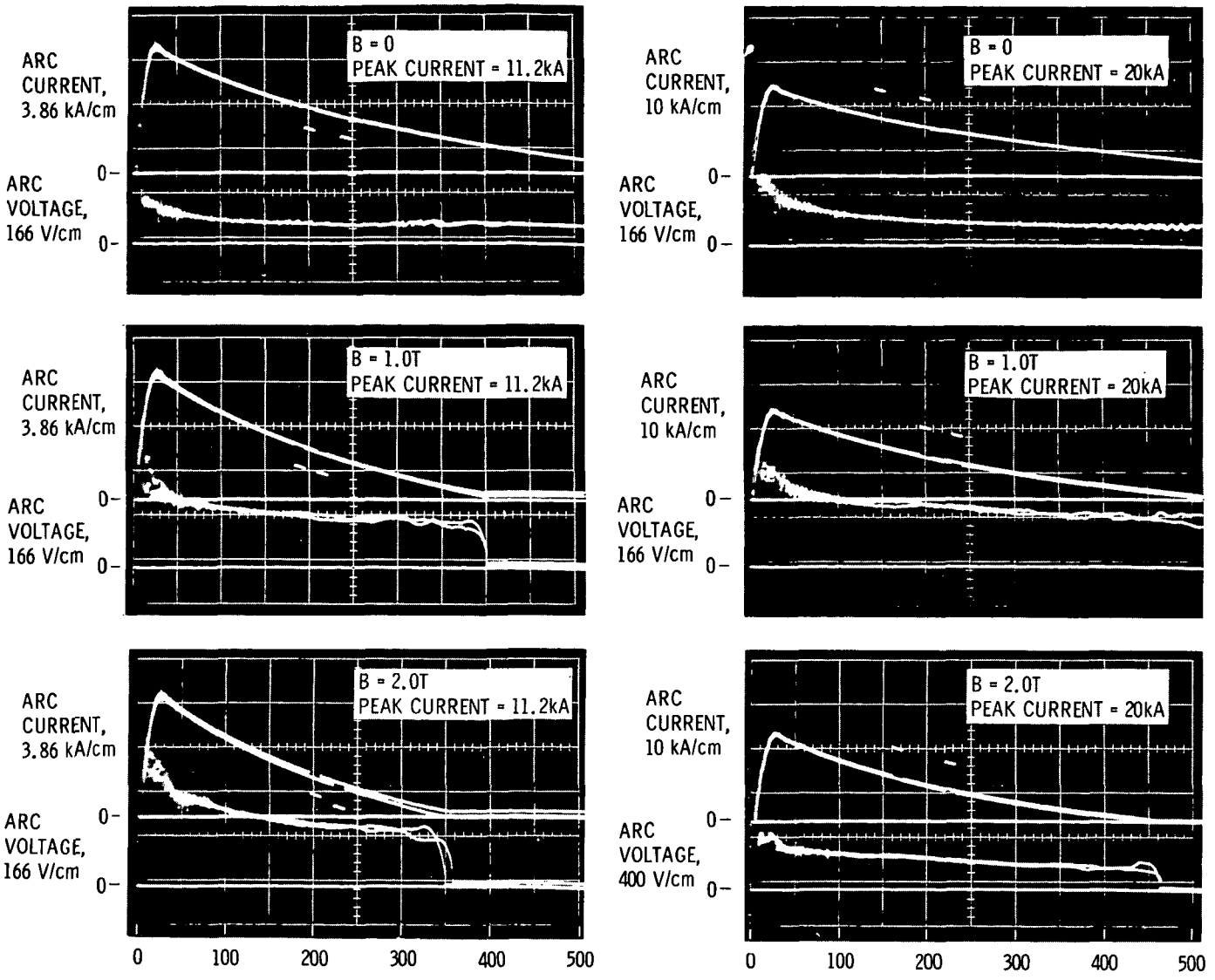

Figure 1. - Current-voltage traces (2-trace overlays).

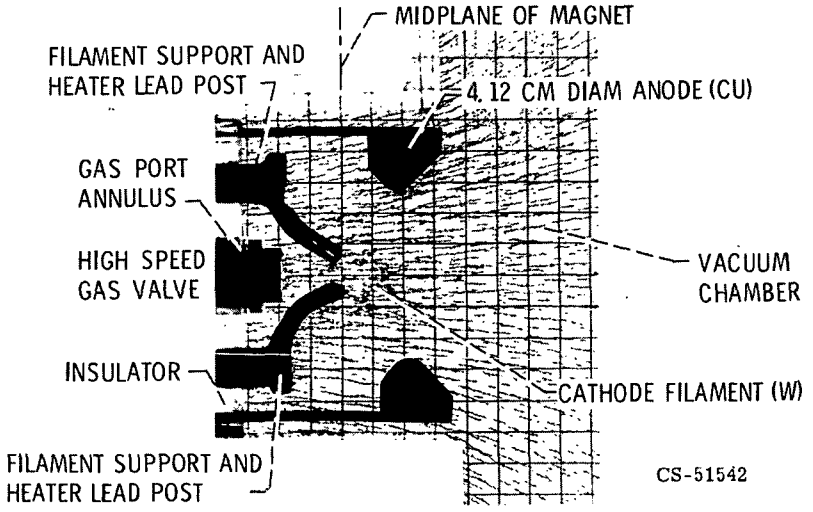

Figure 2. - Arc chamber.

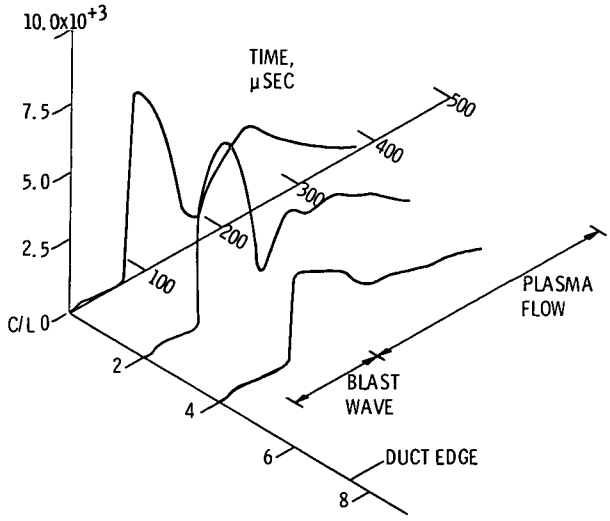

(a) SELF-FIELD CASE.

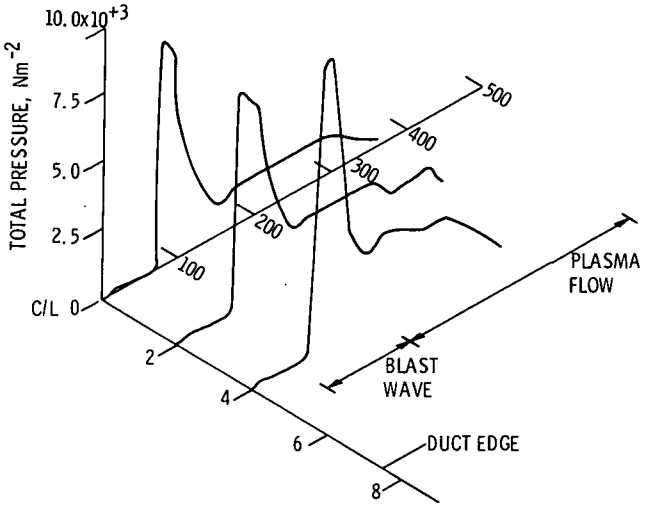

(b) 1.0 T AUXILIARY MAGNETIC FIELD CASE.

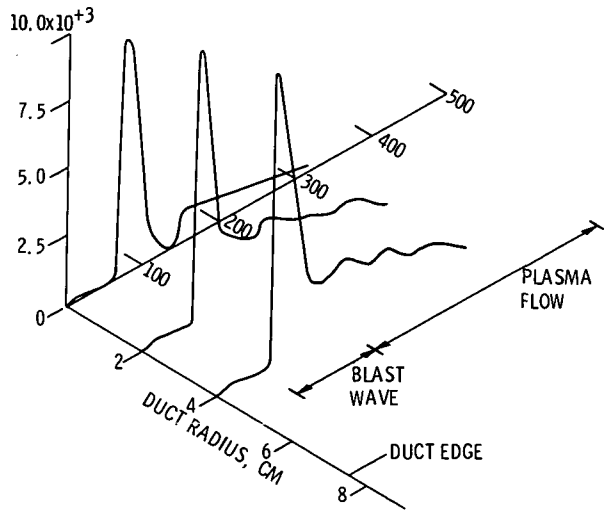

(c) 2.0 T AUXILIARY MAGNETIC FIELD CASE.

Figure 3. - Impact pressure profiles (11.2 kA peak current case).

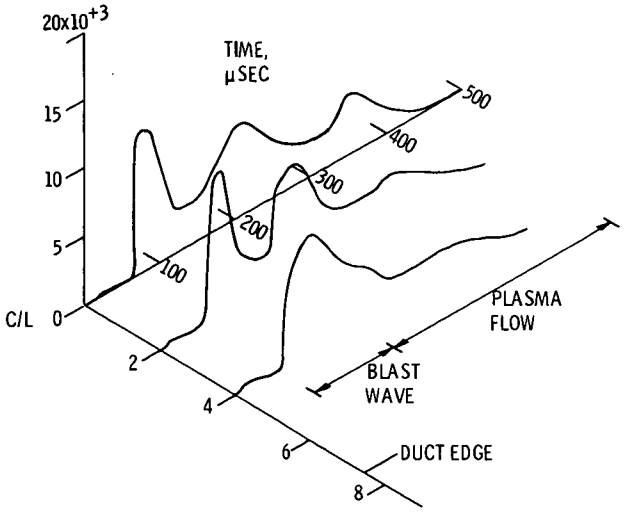

(a) SELF-FIELD CASE.

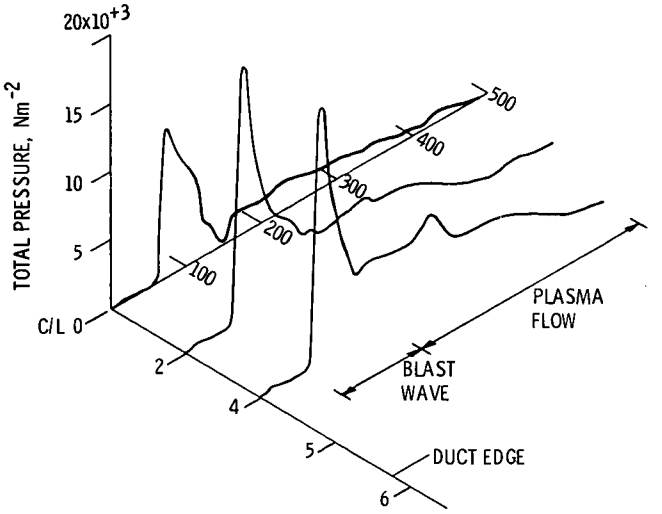

(b) 1.0 T AUXILIARY MAGNETIC FIELD CASE.

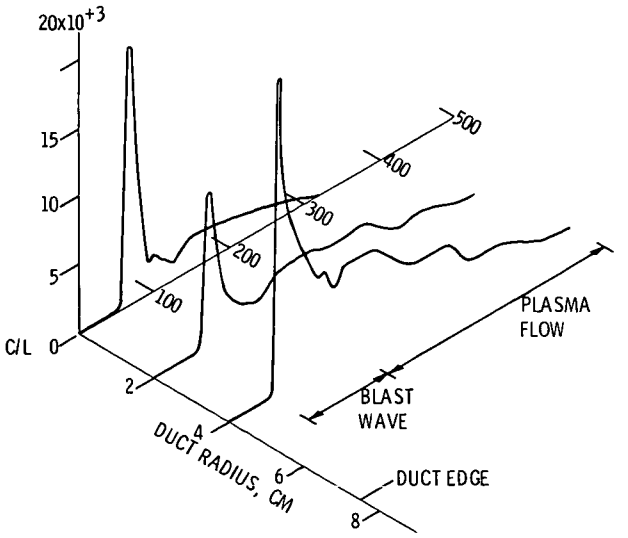

(c) 2.0 T AUXILIARY MAGNETIC FIELD CASE.

Figure 4. - Impact pressure profiles (20.0 kA peak current case).

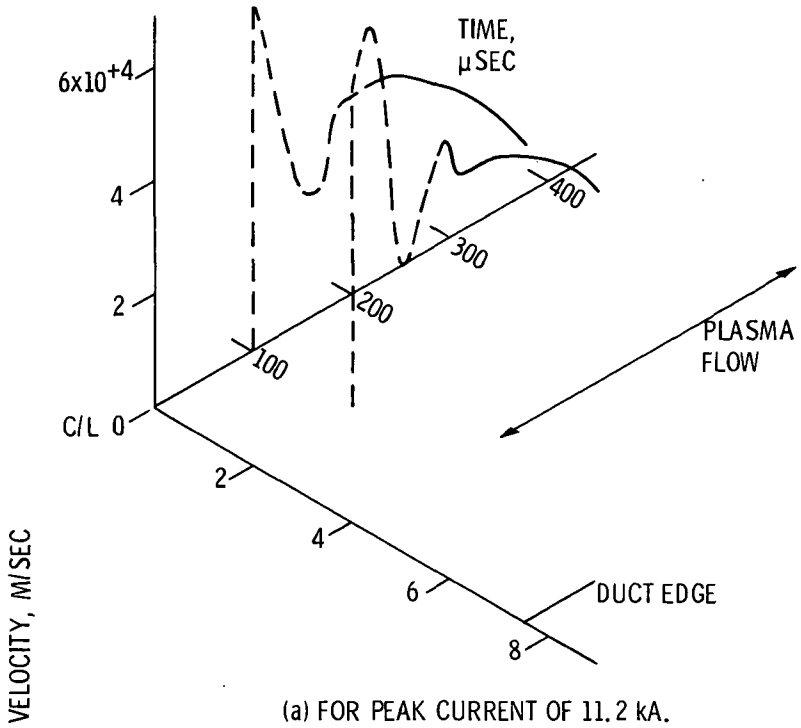

(a) FOR PEAK CURRENT OF 11.2 kA.

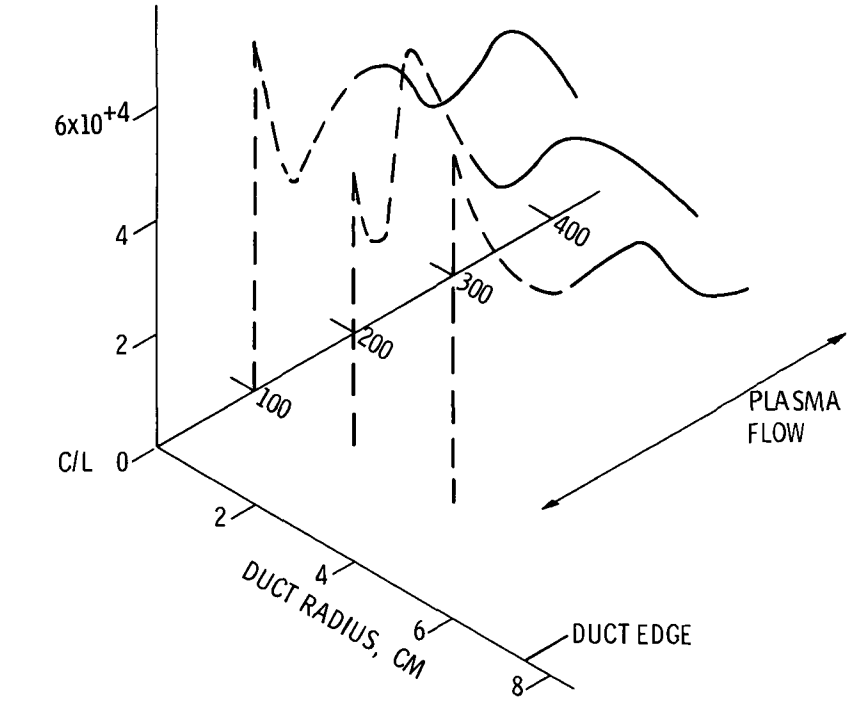

(b) FOR PEAK CURRENT OF 20 kA.

Figure 5. - Velocity profiles (self field case).

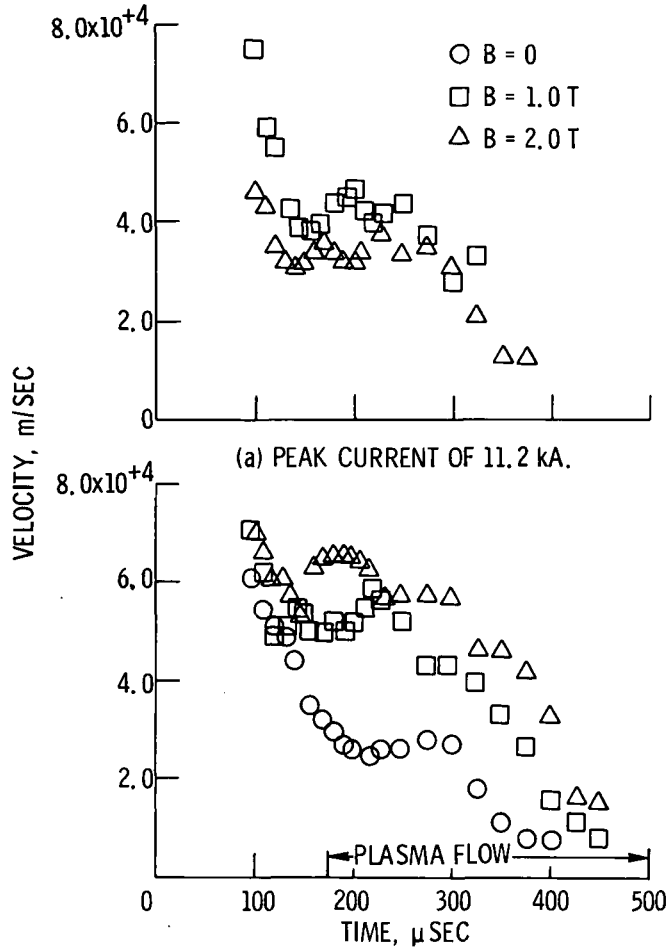

(b) PEAK CURRENT OF 20 kA.

Figure 6. - Velocity versus time (at R = 4 cm, Z = 30 cm).

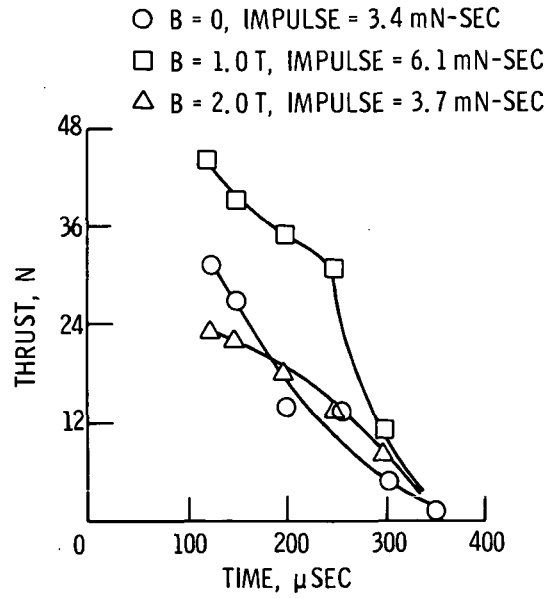

Figure 7. - Instantaneous thrust versus time (peak current of 11.2 kA).

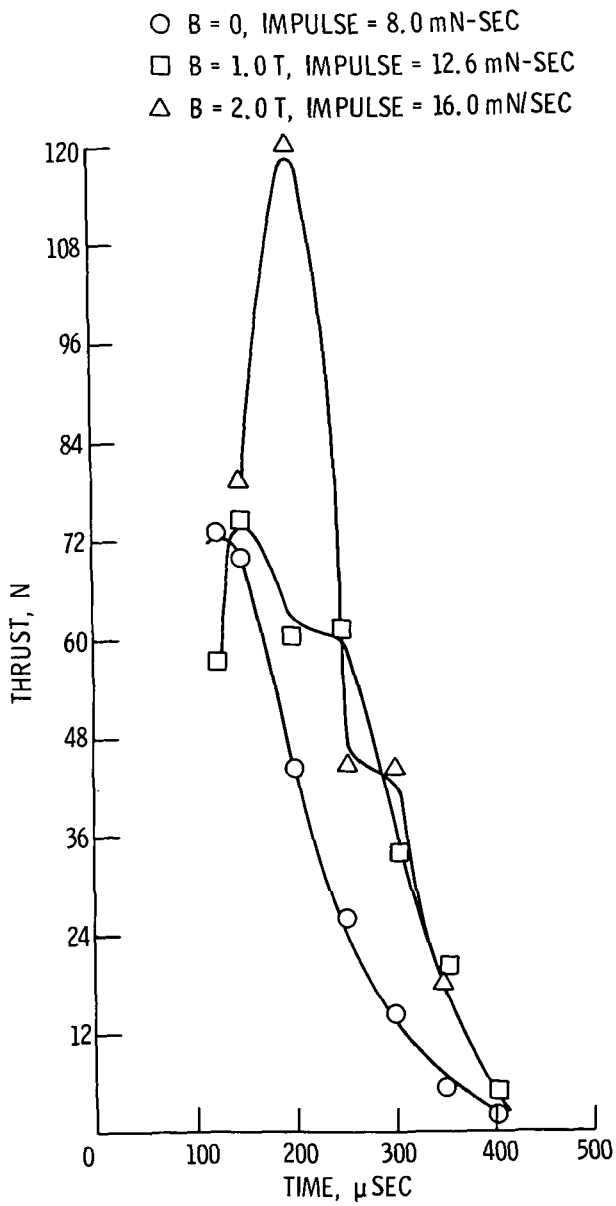

Figure 8. - Instantaneous thrust versus time (peak current of 20 kA).

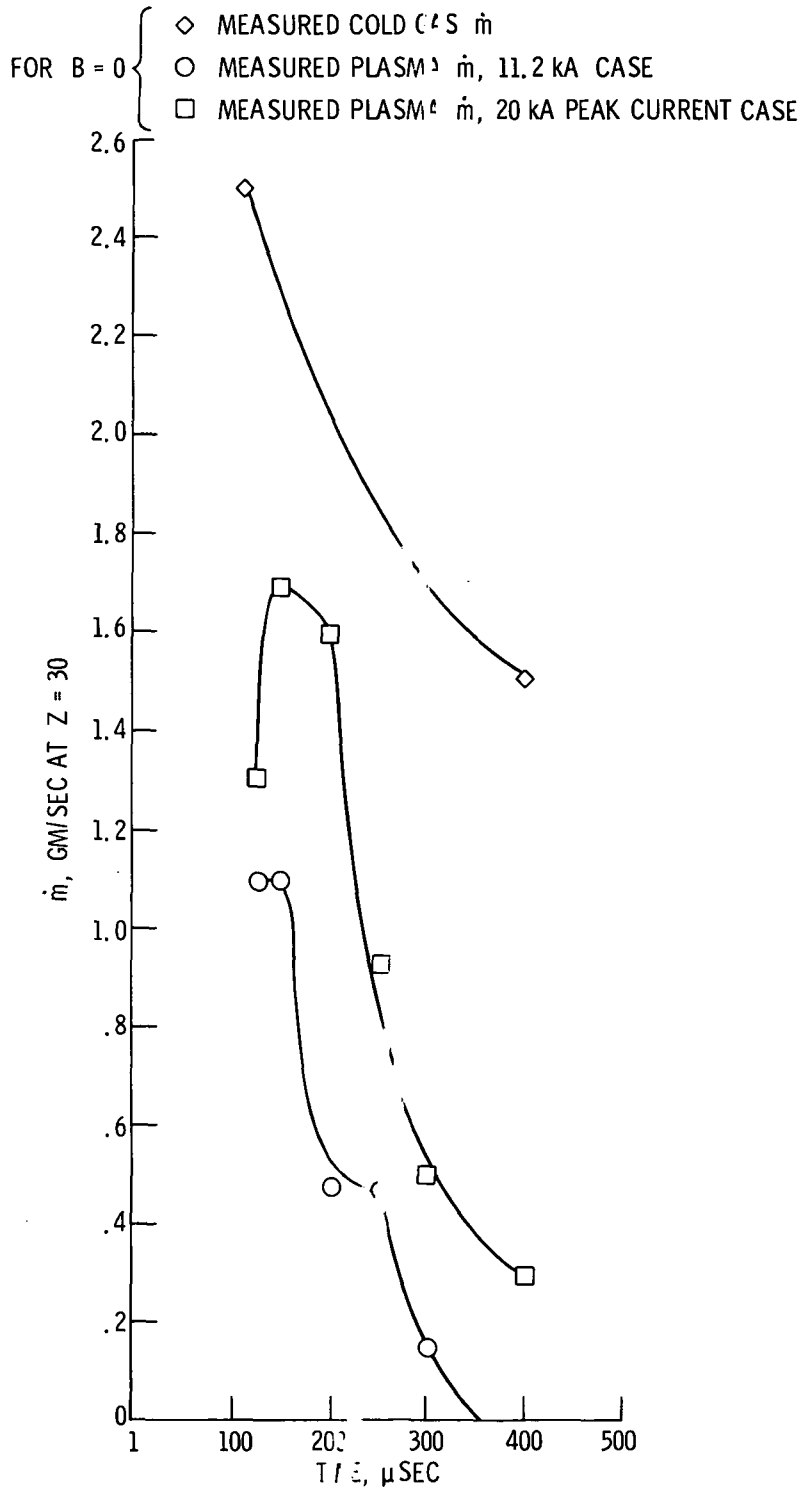

Figure 9. - Instantaneous propellant flow rate.

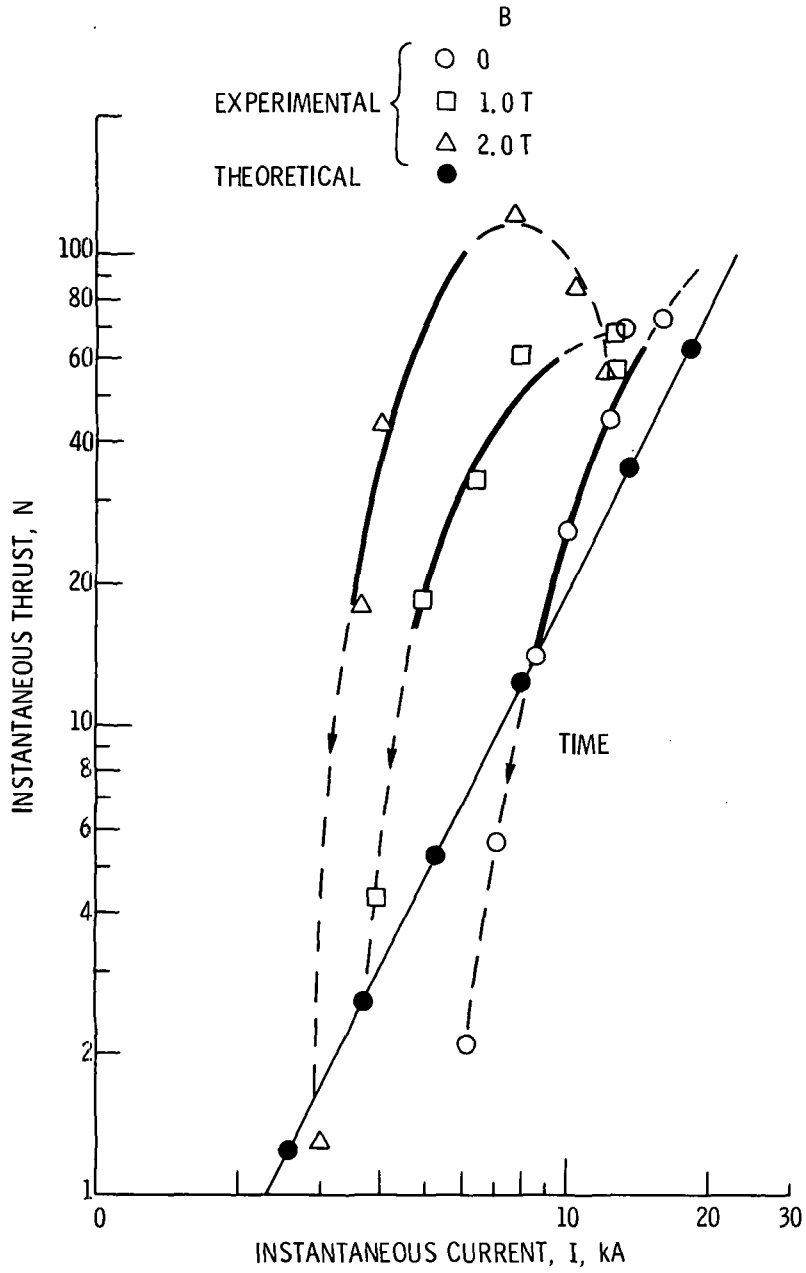

Figure 10. - Instantaneous thrust versus instantaneous current (20.0 kA peak current case).

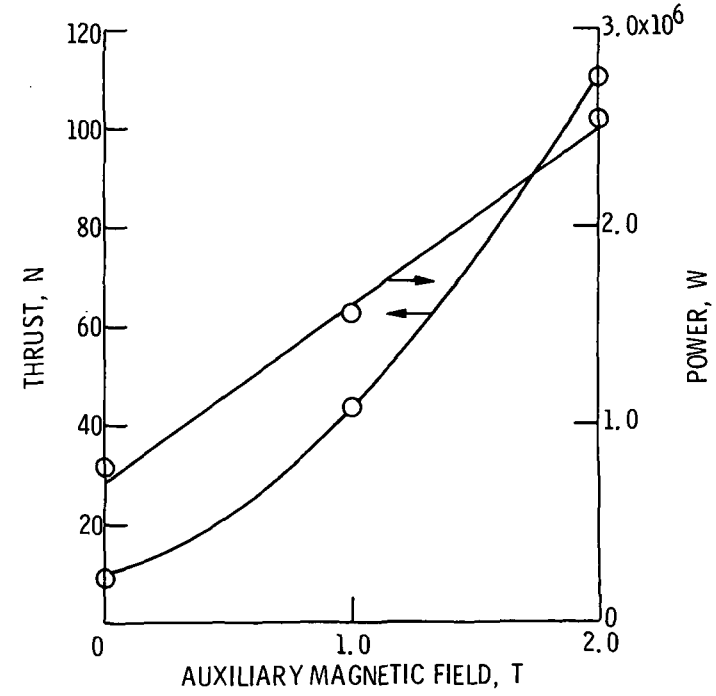

Figure 11. - Thrust and power versus auxiliary magnetic field (current = 8 kA).